

Micro wire electrochemical machining with an axial electrolyte flow

Shaohua Wang · Yongbin Zeng · Yong Liu · Di Zhu

Received: 17 July 2010 / Accepted: 12 December 2011
© Springer-Verlag London Limited 2011

Abstract Micro wire electrochemical machining is a useful technique to produce high-aspect-ratio slit micro-structures. To improve processing stability, the axial electrolyte flow is adopted to renew electrolytes in the machining gap. A wire electrochemical micro-machining system with an axial electrolyte flow unit is developed. A mathematical model of tool feed rate is presented. To investigate the influence of electrolyte flow on processing stability and machining efficiency, comparative experiments were carried out. The influence of applied voltage and electrolyte concentration on machining accuracy is studied and the parameters such as electrolyte flow rate and applied voltage are optimized. Low initial machining gap is applied to decrease the stray current machining in the initial machining period. With the optimal parameters, the high-aspect-ratio micro spline and curved flow channel with the slit width of 160 μm have been fabricated on 5-mm-thick stainless steel (0Cr18Ni9). The width of the slit is uniform and the aspect ratio is 31.

Keywords Electrochemical machining · Micro wire electrode · Axial electrolyte flow · Aspect ratio

1 Introduction

Electrochemical machining (ECM) has recently become popular due its advantages in many applications such as its performance regardless of material hardness and no heat-

affected layer [1]. It can be used to achieve a desired shape of a surface using metal dissolution by electrochemical reaction and can be applied to metals such as high-strength, heat-resistant and hardened steel [2]. The ECM/ECD process originally designed for manufacturing complex shaped components in defense and aerospace industries has been extended to many other industries such as automotive, dies molds, and surgical components [3]. The application of ultrashort voltage pulses between a tool electrode and a work-piece in an electrochemical environment allows the three-dimensional machining of conducting materials with submicrometer precision [4]. Munda and Bhattacharyya [5] reported that electrochemical micromachining (EMM) could be used as one of the best micromachining techniques for machining electrically conducting, tough and difficult-to-machine materials with an appropriate combination of machining parameters. Electrochemistry takes a key position in products and manufacturing processes of microtechnology [6]. Shin et al. [7] have reported that micro wire ECM can be widely applied to micro fabrication of hard alloy metal parts such as micro gears and micro-sized metal parts. Structures with 90 nm width were made by applying 2-ns voltage pulses [8]. Micro ECM has been applied to machining air-lubricated hydrodynamic bearings [9] and various micro-structures on stainless steel [10].

Micro wire ECM is a promising method of EMM. Using a platinum wire electrode with 100 μm diameter, various 3D features were machined on stainless steel plate [10]. By using this method, micro features such as micro grooves and gears were fabricated into stainless steel plates [7]. Zhu et al. [11] reported that many complex micro metal parts with structures of several 10- μm scales were fabricated by micro wire ECM.

However, during production of high-aspect-ratio micro-structures in 5-mm thickness stainless steel by micro wire

S. Wang (✉) · Y. Zeng · Y. Liu · D. Zhu
Research Center for Nontraditional Machining,
College of Mechanical and Electrical Engineering,
Nanjing University of Aeronautics and Astronautics,
Nanjing 210016, China
e-mail: shaohuafei2008@yahoo.cn

ECM, reaction products formed during the machining could not be removed from inter-electrode gap effectively. Bhattacharyya et al. [12] reported that the reaction products between micro-tool and work-piece may cause generation of sparks, which in turn reduces machining accuracy. The high-speed rotary electrode [13] and the intermittently back electrode [14] are possible ways to cleanse electrolytic products and renew electrolyte in machining gap. Because the wire electrode is tensed on a fixture in micro wire ECM, it is difficult to achieve a high-speed rotation of electrodes. Moreover, as the aspect ratio increases, the intermittently back electrode is not effective to cleanse electrolytic products. Thus, both methods are not feasible in micro wire ECM. Forward flow pattern of electrolyte is widely used in ECM. Axial electrolyte flow could cleanse electrolytic products from machining gap effectively and avoid wire electrode vibration. In this research, axial electrolyte flow is adopted to produce high-aspect-ratio slit micro-structures.

2 Principle

Micro wire ECM is similar to common ECM, which is an electrochemical anodic dissolution process. During the machining process, an appropriate voltage is applied between the work-piece and cathode. At the anodic work-piece surface, metal is dissolved into metallic ions by the electrochemical reaction, the micron scale wire tungsten electrode is used as the cathode tool, and following the scheduled tool path, the required shapes or structures can be obtained as shown in Fig. 1. Beyond this, the hydrogen bubbles and sludge is generated during the reaction. Therefore, axial electrolyte flow, whose direction is assumed to be along the axis of the wire electrode, is adapted to renew electrolyte in the machining gap. Combining the axial electrolyte flow, micro wire ECM can be used to fabricate micro parts with the high aspect ratio on metal work-pieces.

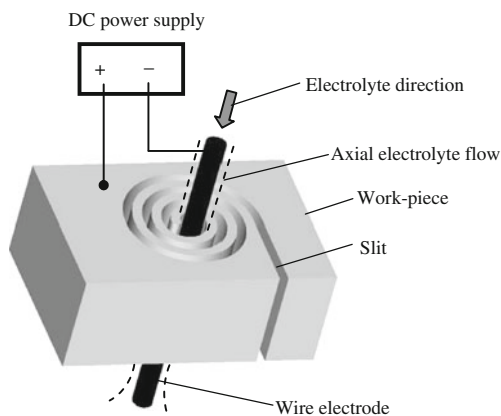


Fig. 1 Schematic diagram of micro wire electrochemical machining

3 Model

The feed rate of wire electrode and the electrolyte flow rate in the pump output mouth (shown in Fig. 2) are modeled. When ECM is in equilibrium state, the cathode feed rate is:

$$v_c = \eta \omega \kappa \frac{U_R}{\Delta_b} \quad (1)$$

where v_c is feed rate of wire electrode, η is the current efficiency, ω is the electrochemical equivalency of anode metal, k is the conductivity of electrolyte and electrolysis product mixture, U_R is the machining voltage, and Δ_b is the inter-electrode frontal gap.

The conductivity of electrolyte and electrolysis product mixture is given by [15]:

$$\kappa = \kappa_0 \frac{2[1 - (\beta_1 + \beta_2)]}{2 + \beta_1 + \beta_2} \quad (2)$$

where κ_0 is the electrolyte conductivity, β_1 is the volume ratio of hydrogen in the electrolyte mixture, and β_2 is the volume ratio of hydroxide in the electrolyte mixture.

The volume ratio of hydrogen and hydroxide is:

$$\beta_1 = \frac{Q_1}{Q_g} \quad (3)$$

$$\beta_2 = \frac{Q_2}{Q_g} \quad (4)$$

where Q_1 is the volume flow of hydrogen through the machining gap, Q_2 is the volume flow of hydroxide through the machining gap, and Q_g is the total volume flow through

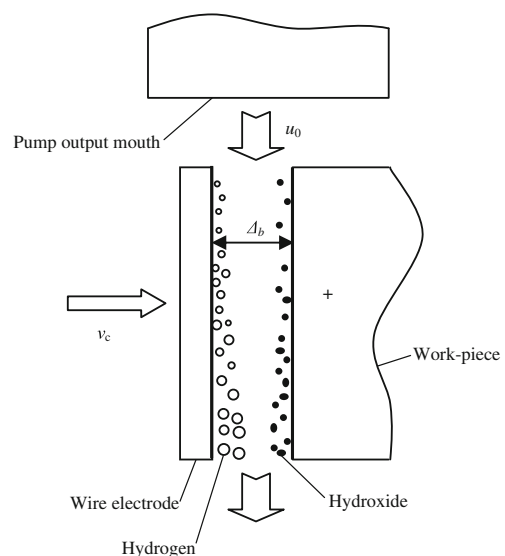
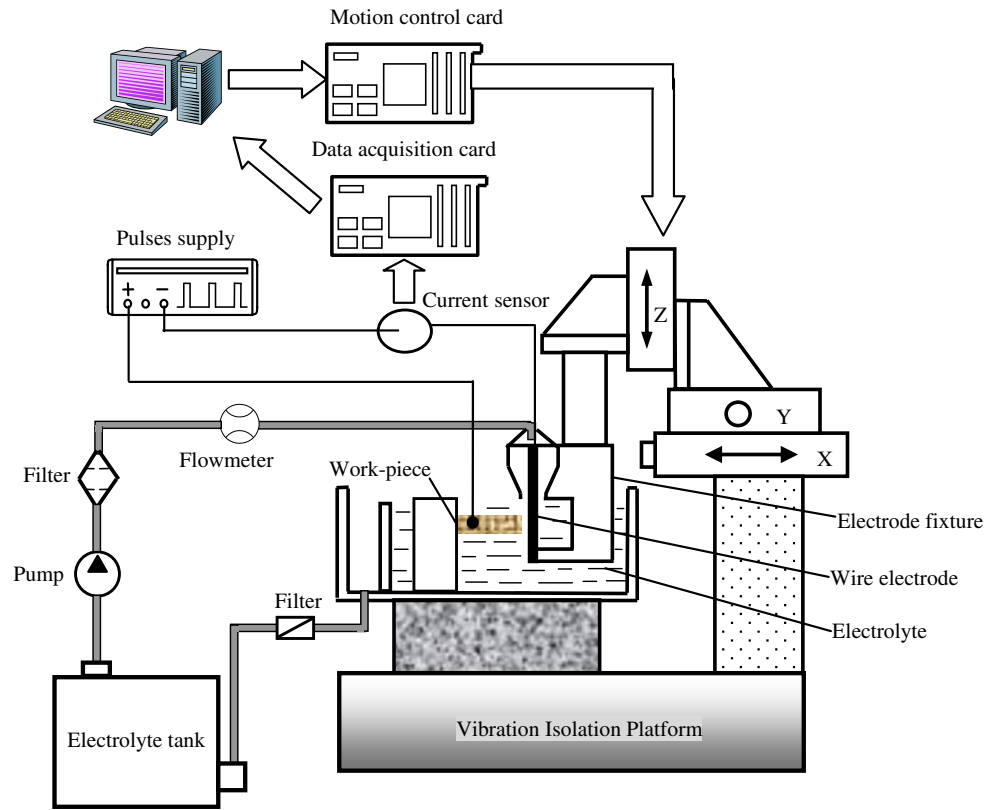


Fig. 2 Sketch of flow field model

Fig. 3 Sketch of experimental system



the machining gap. The pump output volume flow of electrolyte is:

$$Q_p = K_1 K_2 F Q_g \tag{5}$$

where Q_p is the pump output volume flow, K_1 is the overflow coefficient, K_2 is the leakage coefficient, and F is the coefficient of processing surface complexity.

The equation of pump output flow and velocity is:

$$Q_p = u_0 A_0 \tag{6}$$

where u_0 is electrolyte flow rate in pump output mouth and A_0 is the cross-section area of pump output mouth. Substitution of Eq. 6 into Eq. 5 gives:

$$Q_g = \frac{u_0 A_0}{K_1 K_2 F} \tag{7}$$

Solving Eqs. 3, 4 and 7 gives:

$$\beta_1 + \beta_2 = \frac{K_1 K_2 F (Q_1 + Q_2)}{u_0 A_0} \tag{8}$$

From Eqs. 1, 2 and 8, v_c can be obtained:

$$v_c = 2\eta\omega\kappa_0 U_R \frac{u_0 A_0 - K_1 K_2 F (Q_1 + Q_2)}{\Delta_b [2u_0 A_0 + K_1 K_2 F (Q_1 + Q_2)]} \tag{9}$$

From Eq. 9, it is observed that v_c increased as u_0 increased. Electrolyte flow rate is closely related to the feed rate of wire

electrode. Therefore, higher electrolyte flow rate is helpful to improve the machining efficiency.

4 Experimental system and experimental conditions

The self-developed wire electrochemical micro-machining experimental system is shown in Fig. 3. It consists of electrolyte circulation subsystem, machining process detecting subsystem and servo-control feed subsystem. With the C-

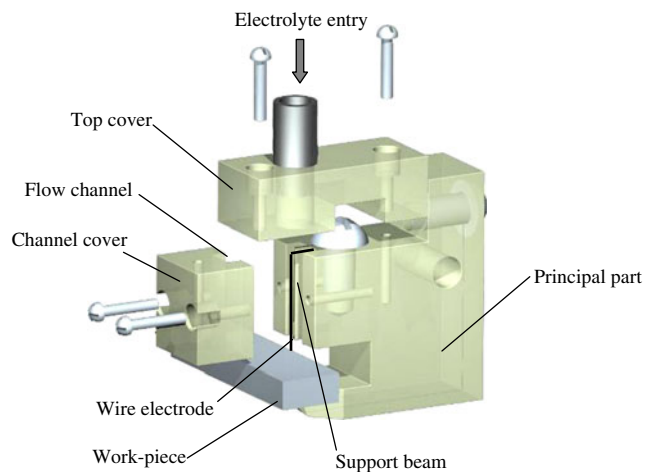


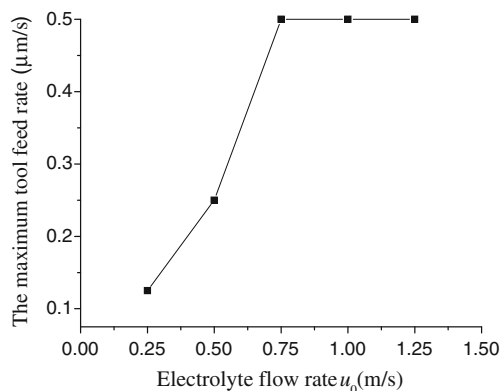
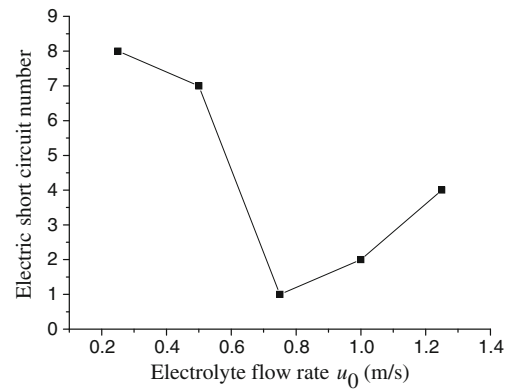
Fig. 4 Sketch of wire electrode fixture

Table 1 Machining parameters for the experiments

Parameter	Value
Electrolyte type	NaNO ₃
Electrolyte temperature	25°C
Flow pattern	Axial electrolyte flow
Electrolyte flow rate	Pump output flow rate, u_0
Work-piece material	0Cr18Ni9
Work-piece thickness	5 mm
Tool material	Tungsten wire
Tool diameter	20 μm

843 motion controller card for core, the servo-control feed subsystem consists of a precise XYZ stage and the software of the machining process control system. The wire electrode is attached to the axes of the feed subsystem. The motion parts of X-, Y- and Z-axes are driven by direct current servo motors through precision ball-race feed screw with resolution of 0.1 μm . The software of control system performs two functions: the trajectory control and the gap control. The control system is developed using the technology of virtual instruments, and the program is based on Lab Windows/CVI.

Figure 4 shows the wire electrode fixture of axial electrolyte flow. The wire electrode fixture is an important part of the machining system. Wire electrode is strained on the principal part of the fixture with screws. Top cover and channel cover are installed on the principal part of the fixture after wire electrode fixed. Support beam is adopted to support wire electrode in flow channel. In order to reduce the influence of the support beam on flow field in the channel, support beam thickness should be as small as possible. For axial electrolyte flow, the electrolyte flow goes gently through the channel along the axial direction of wire

**Fig. 5** The maximum tool feed rate with different pump output electrolyte flow rates (10 V applied voltage; 10 g/l NaNO₃; geometry and length, 800 μm straight slit)**Fig. 6** Number of electric short circuit with different pump output flow rates (10 V applied voltage; 10 g/l NaNO₃; 0.5 $\mu\text{m/s}$ tool feed rate; geometry and length, 800 μm straight slit)

electrode. It is effective to avoid wire electrode vibration caused by the electrolyte flow. During the machining process with an axial electrolyte flow, pump output electrolyte flow rate u_0 is counted according to Eq. 6. The unchanged experimental conditions are shown in Table 1.

5 Experimental results and discussions

5.1 Influence of electrolyte flow rate on wire electrode feed rate

Equation 9 illustrates that wire electrode feed rate increases as the pump output electrolyte flow rate increases. And a higher electrolyte flow rate can improve the machining efficiency. In order to validate the range of applicability and limitations of the theory, comparative experiments are carried. Each flow rate is repeated 20 times, recording the number of electric short circuit. The allowable maximum feed rate with electric short circuit less than twice is accepted as the maximum tool feed rate of the flow rate.

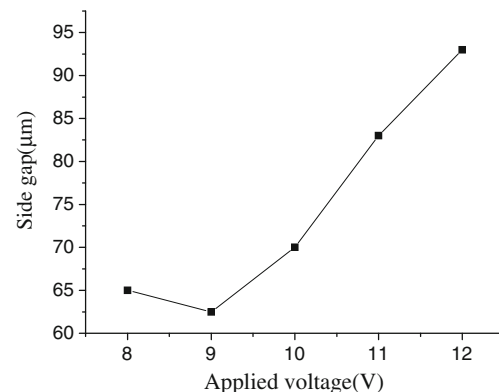
**Fig. 7** Side gap with different applied voltages (10 g/l NaNO₃; pump output flow rate, $u_0=0.75$ m/s; 0.5 $\mu\text{m/s}$ tool feed rate)

Fig. 8 Micro grooves with different applied voltages (10 g/l NaNO_3 ; pump output flow rate, $u_0=0.75$ m/s; $0.5 \mu\text{m/s}$ tool feed rate; applied voltage: **a** 8 V, **b** 10 V, **c** 12 V)

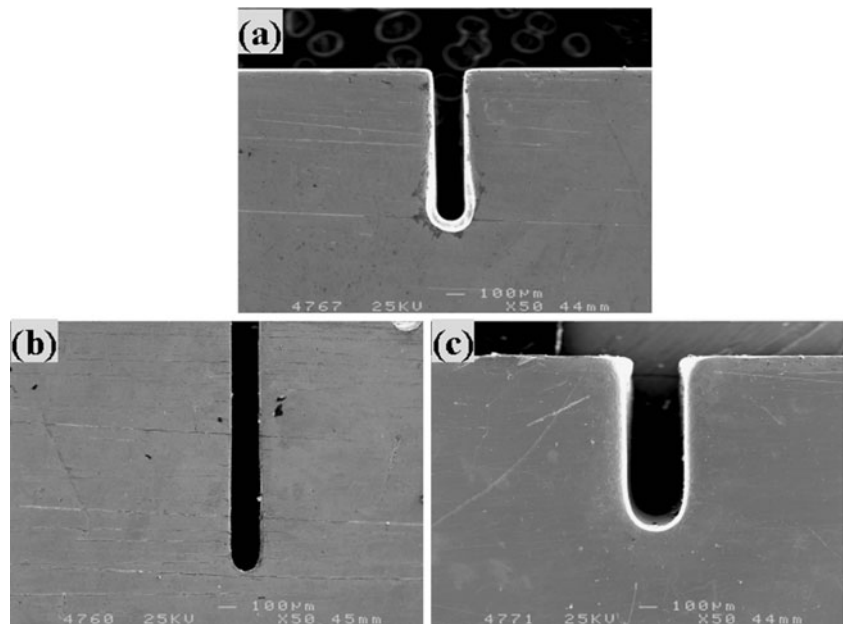


Figure 5 exhibits the influence of pump output flow rate on the maximum tool feed rate without electric short circuit. When the electrolyte flow rate is less than 0.75 m/s, the maximum tool feed rate increased as pump output electrolyte flow rate increased, thus leading the improvement of the machining efficiency. This is because a high flow rate helps to disperse air bubbles and other electrolysis products, and uniform flow field and current density in processing zones, which in turn improves the machining efficiency and the machining stability. The result is in accord with the theory. However, when the tool flow rate is more than 0.75 m/s, the

maximum tool feed rate is no longer increases as the pump output flow rate increases. This is because the inter-electrode frontal gap reduces to a limit as the tool flow rate is above 0.75 m/s. The teeny gap is too small to disperse hydrogen and other electrolysis products, and then the electric short circuit occurs. The result is not applicable to the theory as the tool flow rate is above 0.75 m/s. The conclusion is reached that the range of applicability in Eq. 9 is the tool flow rate below 0.75 m/s. Therefore, considering the machining efficiency and the stable machining with no setback, the optimal tool feed rate is determined to be $0.5 \mu\text{m/s}$.

Fig. 9 Micro grooves with different electrolyte concentrations (10 V applied voltage; pump output flow rate, $u_0=0.75$ m/s; $0.5 \mu\text{m/s}$ tool feed rate; electrolyte concentration: **a** 10 g/l, **b** 20 g/l, **c** 50 g/l)

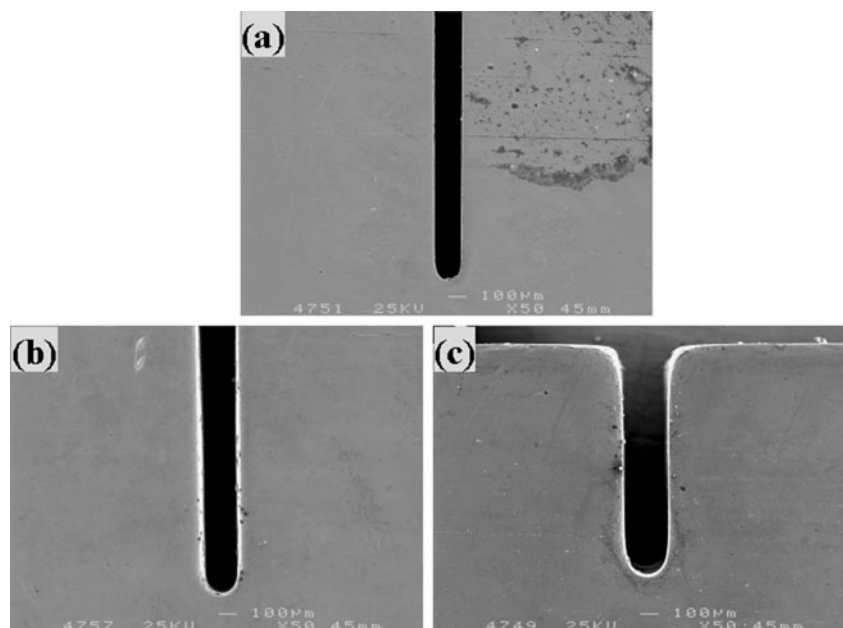
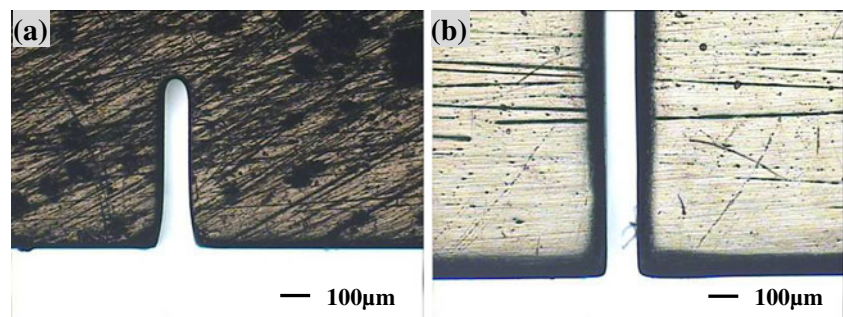


Fig. 10 SEM image of micro groove with stray current attack in the initial machining period (10 V applied voltage; 10 g/l NaNO₃; pump output flow rate, $u_0=0.75$ m/s; 0.5 $\mu\text{m/s}$ tool feed rate; initial machining gap: **a** 100 μm , **b** 60 μm)



5.2 Influence of electrolyte flow rate on machining stability

Figure 6 exhibits the effect of pump output flow rate on machining stability. In the comparative experiments, each process parameter is repeated ten times, recording the number of electric short circuit. The figure shows that the machining stability increased as the electrolyte flow rate increased. However, when the flow rate was higher than 1.0 m/s, electric short circuit between the tool and the work-piece was caused by wire electrode vibration, and the processing stability became worse. Therefore, considering the electrode vibration, the optimal electrolyte flow rate is determined to be 0.75 m/s. This clearly reveals the fact that electrolyte flow rate has a significant effect on the processing stability.

5.3 Influence of applied voltage on machining accuracy

Figure 7 exhibits the effect of applied voltage on side gap with the axial electrolyte flow. The figure shows that the side gap increases as the applied voltage increases. When the applied voltage was 8 V, electric short circuit occurred often due to the low dissolution rate. The machining accuracy is poor as shown in Fig. 8a. When the applied voltage was higher than 8 V, the number of short circuits was reduced to only a few times owing to the larger machining gap which increased as the applied voltage increased. When the applied voltage was 10 V, no electric short circuit was detected. Hence, the machining accuracy becomes better as shown in Fig. 8b. However, when the applied voltage is

12 V, side gap is oversized, and more dissolution occurs at the sides of the groove as shown in Fig. 8c. Therefore, the optimal applied voltage is determined to be 10 V to maintain the stability and uniformity of the machining shape.

5.4 Influence of electrolyte concentration on machining accuracy

There are many factors which have effects on the machining quality in micro wire ECM, such as electrolyte conductivity, current density, and inter-electrode gap. Lee et al. [16] found that electrolyte conductivity, acting as a variable resistance, has been recognized one of the most important parameters in EMM. The lower the electrolyte concentration, the smaller the electrolyte conductivity. As the machining electric current flow becomes smaller, the localized area around the tool narrows down as shown in Fig. 9a. On the contrary, side gap increases with increasing electrolyte concentration, which in turn reduces the machining accuracy as shown in Fig. 9b and c. Therefore, the very dilute sodium nitrate electrolyte is employed to minimize the machining gap and improve the localization of processing. Micro wire ECM with very dilute sodium nitrate of 10 g/l NaNO₃ electrolyte is adopted to improve machining accuracy.

5.5 Stray current attack in the initial machining period

Figure 10 shows a micro groove with stray current attack during the initial machining period. Figure 10a shows that a bell-mouth shape is formed in the groove entrance. In the

Fig. 11 Micro spline on stainless steel (10 V applied voltage; 10 g/l NaNO₃; pump output flow rate)

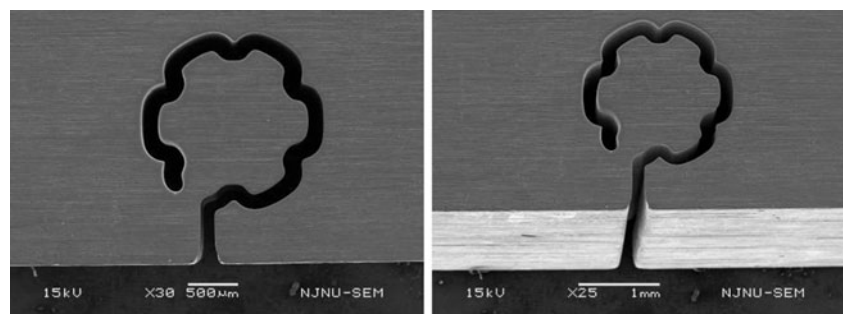
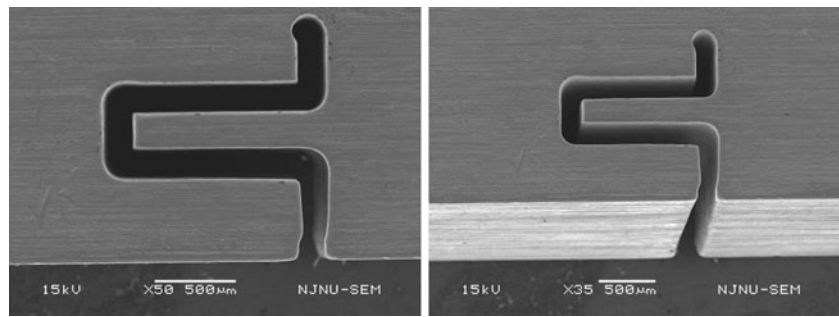


Fig. 12 Micro curved flow channel on stainless steel (10 V applied voltage; 10 g/l NaNO₃; pump output flow rate, $u_0 = 0.75$ m/s; 0.5 $\mu\text{m/s}$ tool feed rate)



initial machining period, the surrounding part of the work-piece, which is far away from the tool, also undergoes dissolution due to electric current lines acting over this zone. Material removal from such areas is called stray current attack [17]. The stray current attack range would be greatly reduced when the electrode advances into the work-piece, owing to the restricting control of the electric current lines by the anode material. As can be seen in Fig. 10b, the bell-mouthed opening can be reduced by decreasing initial machining gap. Thus, a lower initial machining gap can decrease the stray current machining time, resulting in a better entrance shape.

5.6 Fabrication of complex micro-structure

With the axial electrolyte flow, micro-structures were machined. Figure 11 shows a micro spline structure with the slit width of 160 μm on a 5-mm-thick stainless steel. Figure 12 shows a micro curved flow channel with the slit width of 160 on a 5-mm-thick stainless steel. The width of the slits is uniform, and the aspect ratio is 31. The work-piece, except the etched groove, has an innate surface due to the localization of the machining region. During the machining, no contact between the tool and the work-piece was detected and the groove's width remained constant.

6 Conclusion

This paper reports the influence of electrolyte flow on micro wire ECM. The following conclusions can be drawn based on the experiments and discussions mentioned above:

1. Axial electrolyte flow is adopted to be the optimal flow pattern for micro wire ECM.
2. Through theoretical analysis and comparative experiments, it is revealed that processing stability and machining efficiency can be improved by a higher electrolyte flow rate. And the conclusion is reached that the range of applicability of Eq. 9 is the tool flow rate below 0.75 m/s.
3. Optimized process parameters of 1.0 m/s electrolyte flow rate, 10 V applied voltage and 10 g/l NaNO₃ electrolyte are achieved under an axial electrolyte flow condition. Better machining accuracy can be achieved by the optimized process parameters.
4. Lower initial machining gap can decrease the stray current machining time, resulting in a better entrance shape.
5. With optimized parameters, structures of micro curved flow channel and micro spline with the aspect ratio of 31 were fabricated on 5-mm-thick stainless steel. As can be seen from the experimental results and SEM micrographs, the machining accuracy is improved by the axial electrolyte flow.

Acknowledgments The authors acknowledge the financial support provide by the China Natural Science Foundation (50635040), the National High-tech Research and Development Program (2009AA04Z302) and Jiangsu Provincial Natural Science Foundation (BK2008043).

References

1. Bhattacharyya B, Doloi B, Sridhar PS (2001) Electrochemical micro-machining: new possibilities for micro-manufacturing. *J Mater Process Technol* 113(1–3):301–305
2. Lee ES, Park JW, Moon YH (2002) A study on electrochemical micromachining for fabrication of microgrooves in an air-lubricated hydrodynamic bearing. *Int J Adv Manuf Technol* 20(10):720–726
3. Amalnik MS, McGeough JA (1996) Intelligent concurrent manufacturability evaluation of design for electrochemical machining. *J Mater Process Technol* 61(1–2):130–139
4. Schuster R, Kirchner V, Allongue P, Ertl G (2000) Electrochemical micromachining. *Science* 289(5476):98–101
5. Munda J, Bhattacharyya B (2008) Investigation into electrochemical micromachining (EMM) through response surface methodology based approach. *Int J Adv Manuf Technol* 35(7–8):821–832
6. Ehrfeld W (2003) Electrochemistry and microsystems. *Electrochim Acta* 48(20–22):2857–2868
7. Shin HS, Kim BH, Chu CN (2008) Analysis of the side gap resulting from micro electrochemical machining with a tungsten wire and ultrashort voltage pulses. *J Micromech Microeng* 18(7):1–6

8. Trimmer AL, Hudson JL, Kock M, Schuster R (2003) Single-step electrochemical machining of complex nanostructures with ultrashort voltage pulses. *Appl Phys Lett* 82(19):3327–3329
9. Park JW, Lee ES, Won CH, Moon YH (2003) Development of electrochemical micromachining for air-lubricated hydrodynamic bearings. *Microsyst Technol* 9(1–2):61–66
10. Kim BH, Na CW, Lee YS, Choi DK, Chu CN (2005) Micro electrochemical machining of 3D micro structure using dilute sulfuric acid. *Ann CIRP* 54(1):191–194
11. Zhu D, Wang K, Qu NS (2007) Micro wire electrochemical machining by using in situ fabricated wire electrode. *Ann CIRP* 56(1):241–244
12. Bhattacharyya B, Malapati M, Munda J, Sarkar A (2007) Influence of tool vibration on machining performance in electrochemical micro-machining of copper. *Int J Mach Tools Manuf* 47(2):335–342
13. Li Y, Zheng YF, Yang G, Peng LQ (2003) Localized electrochemical micromachining with gap control. *Sens Actuators A* 108(1–3):144–148
14. Bhattacharyya B, Munda J (2003) Experimental investigation on the influence of electrochemical machining parameters on machining rate and accuracy in micromachining domain. *Int J Mach Tools Manuf* 43(13):1301–1310
15. Wang JY, Xu JW (2001) Principle and application of electrochemical machining. National Defense Industry Press, Beijing, pp 51–52 [in Chinese]
16. Lee ES, Baek SY, Cho CR (2007) A study of the characteristics for electrochemical micromachining with ultrashort voltage pulses. *Int J Adv Manuf Technol* 31(7–8):762–769
17. Jain VK, Kanetkar Y, Lal GK (2005) Stray current attack and stagnation zones in electrochemical drilling. *Int J Adv Manuf Technol* 26(5):527–536